

Two Novel Coordination Polymers: Synthesis, Structure, Luminescent Properties, and Selective Sensing of Cu²⁺ and Mn²⁺ Ions¹

C. Lian, X. Guo, Y. S. Long, and L. R. Yang*

Henan Key Laboratory of Polyoxometalates, College of Chemistry and Chemical Engineering, Henan University,
Kaifeng, 475004 P.R. China

*e-mail: lirongyang@henu.edu.cn

Received February 3, 2016

Abstract—Two novel coordination polymers, namely $\{[\text{Co}(\text{Ttac})_{0.5}(1,4\text{-Bib})(\text{H}_2\text{O})] \cdot \text{H}_2\text{O}\}_n$ (**I**) and $\{[\text{La}(\text{HTtac})_2(\text{H}_2\text{O})] \cdot \text{H}_2\text{O}\}_n$ (**II**) (H_4Ttac = 4,5-di(3'-carboxylphenyl)-phthalic acid, 1,4-Bib = 1,4-bis(1-imidazolyl)benzene), have been designed and successfully prepared via hydrothermal process, and characterized by elemental analyses, IR spectroscopy, and single crystal X-ray diffraction (CIF files CCDC nos. 1039298 (**I**), 1039300 (**II**)). Structural analysis reveals that the H_4Ttac ligands adopt different coordination modes in the as-synthesized **I** and **II**, and thus give rise to the targeted coordination polymers with different configurations. It is worth mentioning that, coordination polymer **I** is assembled from low-dimensional structures into three-dimensional (3D) via $\pi \cdots \pi$ stacking interactions, while three-dimensional coordination polymer **II** is formed by covalent bonds. Luminescent properties of coordination polymer **II** have been studied at ambient temperature. Significantly, luminescent measurement indicates that coordination polymer **II** may be acted as potential luminescent recognition sensors towards Cu²⁺ and Mn²⁺ ions.

Keywords: hydrothermal synthesis, coordination polymers, luminescent properties, recognition, metal-organic frameworks

DOI: 10.1134/S1070328417050037

INTRODUCTION

Over the past decades, coordination polymers consisting of metal ions or clusters as nodes and organic ligands as linkers have become one of the fastest growing fields in chemistry and attract immense interest not only due to their intriguing structural architectures, but also for their novel characteristics of high surface areas, tailored pore size and functionality [1–4], which make coordination polymers own potentially industrial applications in gas storage and separation, catalysis, magnetism, drug delivery molecular sensing, as well as selective luminescent probes due to their high sensitivity, and quick response [5–10].

As coordination polymers are built on the inherent strong coordination of the linker to the metal centers, a wide variety of structures are accessible, under the condition of the appropriate temperature, acidity, and solvent, rational design and judicious selection of suitable ligands play an critical role in the formation of the coordination frameworks with controlled pore size, shape, and functionality for specific applications [11–

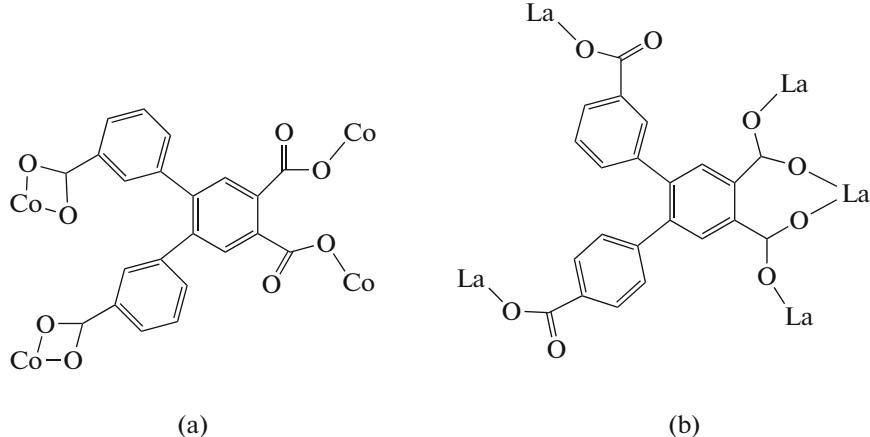
13]. Aromatic polycarboxylates have been convinced as good candidates in the construction of targeted coordination polymers because the flexible ligands may adopt various coordination modes in the crystallization and further lead to structural isomerism. On the other hand, nitrogen-containing auxiliary ligands also have been frequently chosen in the preparation of high dimensional structure, which containing pyridine and imidazole rings are more conducive to form hydrogen-bonding and $\pi \cdots \pi$ stacking interactions that have great impacts on affording extended open frameworks via polymerization [14, 15].

In this paper, we selected a flexible symmetric multidentate tetracarboxylic acid, namely 4,5-di(3'-carboxylphenyl)-phthalic acid (H_4Ttac), nitrogen-containing auxiliary ligands 1,4-bis(1-imidazolyl)benzene (1,4-Bib) and 4,4'-bis(imidazolyl) biphenyl (4,4'-Bibp) together with different metal centers by adjusting pH value and temperature; two different coordination polymers have been prepared successfully, which are formulated as $\{[\text{Co}(\text{Ttac})_{0.5}(1,4\text{-Bib})] \cdot 2\text{H}_2\text{O}\}_n$ (**I**), and $\{[\text{La}(\text{HTtac})_2(\text{H}_2\text{O})]\}_n$ (**II**). We report their synthe-

¹ The article is published in the original.

ses, structures and characterization by elemental analyses, IR spectra, and single-crystal X-ray diffraction. Moreover, the luminescent properties of **II**

have been performed. The coordination modes of H_4Ttac ligand in the coordination polymers **I** (a) and **II** (b) are illustrated in Scheme:



EXPERIMENTAL

Reagents and general techniques. All chemicals were commercially purchased and used without further purification. Elemental analyses (C, H, and N) were performed on a Perkin-Elmer 2400-II CHNS/O analyzer. IR spectra in the range of 400–4000 cm^{-1} were recorded with an AVATAR 360 FT-IR spectrometer using KBr pellets. Photoluminescence spectra and lifetime were measured with an Edinburgh FLS 980 analytical instrument.

Synthesis of I. H_4Ttac (406 mg, 0.1 mmol), 1,4-Bib (210 mg, 0.1 mmol) and cobalt perchlorate hydrate (734 mg, 0.2 mmol) were mixed in water (8 mL), then the mixture was homogenized by stirring for 30 min, and transferred into 25 mL Teflon-lined stainless steel autoclave under autogenous pressure at 140°C for 3 days. After cooling the reaction system to room temperature at a rate of 5°C/h, block red crystals were isolated, washed with distilled water and dried in air at ambient temperature. The yield was 20.31% (based on cobalt perchlorate hydrate).

For $\text{C}_{23}\text{H}_{21}\text{N}_4\text{O}_7\text{Co}$

anal. calcd., %: C, 52.25; H, 4.01; N, 10.89.
Found, %: C, 52.68; H, 4.04; N, 10.68.

IR data (ν , cm^{-1}): 3425 b, 3146 w, 2925 w, 1609 s, 1529 s, 1401 s, 1307 m, 1266 w, 1133 m, 1066 s, 960 m, 937 w, 829 m, 778 s, 701 w, 654 m, 509 w.

Synthesis of II. H_4Ttac (305 mg, 0.75 mmol), benzene 4,4'-bis(imidazolyl) biphenyl (215 mg, 0.75 mmol) and lanthanum nitrate (325 mg, 0.75 mmol) were mixed in water (10 mL), then the mixture was homogenized by stirring for 30 min, and

transferred into 25 mL Teflon-lined stainless steel autoclave under autogenous pressure at 140°C for 3 days. After cooling the reaction system to room temperature at a rate of 5 K/h, colorless block crystals were isolated, washed with distilled water and dried in air at ambient temperature. The yield was 38.93% (based on lanthanum nitrate).

For $\text{C}_{22}\text{H}_{17}\text{O}_{11}\text{La}$

anal. calcd., %: C, 45.39; H, 2.81.
Found %: C, 44.31; H, 2.87.

IR data (ν , cm^{-1}): 3636 b, 3375 w, 2925 w, 2499 w, 1650 w, 1584 m, 1598 m, 1553 s, 1535 m, 1403 s, 1346 m, 1260 m, 1167 w, 1085 w, 912 m, 807 m, 767 s, 708 m, 685 w, 563 m, 509 w, 493 m.

X-ray structure determination. The crystal structure of coordination polymers **I** and **II** were measured on a Bruker Smart CCD X-ray single-crystal diffractometer with graphite monochromated MoK_α -radiation ($\lambda = 0.71073 \text{ \AA}$) at 293(2) K. All independent reflections were collected in a range of 2.98°–26.37° for **I** and 3.20°–26.37° for **II**. The crystal structure was solved by direct methods and Fourier synthesis. Positional and thermal parameters were refined by the full-matrix least-squares method on F^2 using the SHELXTL software package, multi-scan empirical absorption corrections were applied to the data using the SADABS. The key crystallographic date of compound **I** and **II** is given in Table 1. Selected bond lengths and band angles are listed in Table 2. Supplementary materials have been deposited with the Cambridge Crystallographic Data Centre (nos. 1039298 (**I**) and 1039300 (**II**) deposit@ccdc.cam.ac.uk or <http://www.ccdc.cam.ac.uk>).

Table 1. Summary of crystallographic data for coordination polymers **I** and **II**

Parameter	Value	
	I	II
Formula weight	524.37	594.25
Crystal system	Monoclinic	Triclinic
Space group	<i>C</i> 2/c	<i>P</i> 1
<i>a</i> , Å	13.1808(5)	9.0265(5)
<i>b</i> , Å	24.0569(8)	9.8280(5)
<i>c</i> , Å	14.3173(6)	13.0303(6)
α, deg	90.00	106.928(4)
β, deg	95.387(4)	104.677(4)
γ, deg	90.00	95.355(4)
Volume, Å ³	4519.8(3)	1052.20(9)
<i>Z</i>	4	2
ρ _{calcd.} , /cm ³	1.541	1.876
μ, mm ⁻¹	0.813	2.095
<i>F</i> (000)	2160	584
2θ Range for data collection, deg	5.96–52.74	6.40–52.74
Index ranges	–16 ≤ <i>h</i> ≤ 15, –29 ≤ <i>k</i> ≤ 30, –15 ≤ <i>l</i> ≤ 17	–11 ≤ <i>h</i> ≤ 11, –12 ≤ <i>k</i> ≤ 12, –16 ≤ <i>l</i> ≤ 15
Reflections collected	13487	12869
Independent reflections (<i>R</i> _{int})	4606 (0.0388)	4297 (0.0417)
Independent parameters	323	313
Goodness-of-fit on <i>F</i> ²	1.025	1.194
Final <i>R</i> indexes (<i>I</i> ≥ 2σ(<i>I</i>))	<i>R</i> ₁ = 0.0483, <i>wR</i> ₂ = 0.0926	<i>R</i> ₁ = 0.0384, <i>wR</i> ₂ = 0.0895
Final <i>R</i> indexes (all data)	<i>R</i> ₁ = 0.0663, <i>wR</i> ₂ = 0.1008	<i>R</i> ₁ = 0.0423, <i>wR</i> ₂ = 0.0910
Largest diff. peak/hole, <i>e</i> Å ⁻³	0.513/–0.524	1.763/–0.691

RESULTS AND DISCUSSION

The structure of coordination polymers **I** and **II** are identified by X-ray analyses and characterized by satisfactory elemental analysis as well as FT-IR. The coordination polymer **I** has broad band around 3425 cm⁻¹ and peak at 937 cm⁻¹, which due to water molecules in coordination and lattice forms [16]. The strong and broad absorption bands in the region of 1609 and 1529 cm⁻¹ may be ascribed to the asymmetric (COO⁻), and the absorption band at 1401 cm⁻¹ represents the symmetric (COO⁻) stretching of carboxyl groups from Ttac⁴⁻ ligands. The values of Δ(ν_{as} - ν_s) are about 208 and 128 cm⁻¹, respectively, which indicates that the carboxyl groups are coordinated with the metal ions via monodentate and bidentate mode [17, 18]. The absence of the characteristic band around 1700 cm⁻¹ shows the H₄Ttac ligands are completely deprotonated in the form of Ttac⁴⁻ anions upon the coordination with Co²⁺ ion [19]. The

coordination polymer **II** has broad bands around 3375 cm⁻¹ and peak at 912 cm⁻¹, which may be ascribed to water molecules in coordination and lattice forms. The strong broad absorption bands in the region of 1650 and 1403 cm⁻¹ may be ascribed to the asymmetric (COO⁻) and symmetric (COO⁻) stretching of carboxyl groups of Ttac⁴⁻ ligands. The absence of the characteristic bands around 1700 cm⁻¹ is attributed to that the H₄Ttac ligands are completely deprotonated in the form of Ttac⁴⁻ anions upon the reaction with La³⁺ ion. The same conclusions are also supported by the results obtained from X-ray diffraction measurements.

In coordination polymer **I**, each central Co(II) is six-coordinated by three oxygen atoms (O(3), O(4), and O(5)) belonging to two Ttac⁴⁻ ligands, two nitrogen atoms (N(1) and N(4)) from two 1,4-Bib ligands, as well as one terminal water molecule (O(5w)), giving a distorted octahedral coordination geometry

Table 2. Selected bond lengths (Å) and band angles (deg) for the coordination polymers **I** and **II**

Bond	<i>d</i> , Å	Bond	<i>d</i> , Å	Bond	<i>d</i> , Å
I					
Co(1)–O(1)	2.0982(18)	Co(1)–O(5)	2.142(2)	Co(1)–N(1)	2.101(2)
Co(1)–N(4)	2.107(2)	Co(1)–O(3)	2.2635(18)	Co(1)–O(4)	2.109(2)
II					
La(1)–O(31)	2.392(4)	La(1)–O(28)	2.425(4)	La(1)–O(27)	2.574(4)
La(1)–O(16)	2.461(4)	La(1)–O(32)	2.542(4)	La(1)–O(30)	2.463(4)
La(1)–O(24)	2.497(4)	La(1)–O(34)	2.572(4)		
Angle	ω , deg		Angle		ω , deg
I					
O(1)Co(1)O(5)	93.85(8)	N(1)Co(1)(O3)	85.48(8)		
O(1)Co(1)N(1)	96.02(8)	N(1)Co(1)(O4)	94.30(8)		
O(1)Co(1)N(4)	93.26(8)	N(4)Co(1)(O5)	87.44(9)		
O(1)Co(1)O(3)	150.50(7)	N(4)Co(1)(O3)	88.94(8)		
O(1)Co(1)O(4)	90.43(7)	N(4)Co(1)(O4)	90.69(9)		
O(5)Co(1)O(3)	115.64(7)	O(4)Co(1)(O5)	175.42(7)		
N(1)Co(1)O(5)	86.88(9)	O(4)Co(1)(O3)	60.12(6)		
N(1)Co(1)N(4)	169.42(9)				
II					
O(31)La(1)O(28)	139.87(13)	O(28)La(1)O(24)	75.64(13)		
O(31)La(1)O(27)	67.27(12)	O(28)La(1)O(34)	67.54(14)		
O(31)La(1)O(16)	108.32(15)	O(16)La(1)O(27)	73.03(15)		
O(31)La(1)O(32)	69.50(14)	O(16)La(1)O(32)	154.16(15)		
O(31)La(1)O(30)	82.78(13)	O(16)La(1)O(30)	79.22(15)		
O(31)La(1)O(24)	140.06(13)	O(16)La(1)O(24)	96.25(16)		
O(31)La(1)O(34)	87.41(14)	O(16)La(1)O(34)	137.61(15)		
O(28)La(1)O(27)	76.82(13)	O(32)La(1)O(27)	125.22(13)		
O(28)La(1)O(16)	76.17(14)	O(32)La(1)O(34)	68.07(15)		
O(28)La(1)O(32)	122.94(15)	O(30)La(1)O(27)	129.09(13)		
O(28)La(1)O(30)	135.81(13)	O(30)La(1)O(32)	74.96(15)		
O(30)La(1)O(24)	71.23(13)	O(24)La(1)O(32)	74.68(14)		
O(30)La(1)O(34)	142.87(14)	O(24)La(1)O(34)	95.29(15)		
O(24)La(1)O(27)	152.14(12)	O(24)La(1)O(27)	77.91(14)		

(Fig. 1a). The Co–O and Co–N bond lengths are in the range of 2.098–2.264 and 2.107–2.142 Å, respectively. The angles of OCoO are within the scopes of 60.12(6)°–175.42(7)° (Tables 1 and 2). Each completely deprotonated Ttac⁴⁻ ligand links to four Co²⁺ ions using its four carboxyl groups that employs a complicated coordination mode (Scheme, a), and each N-donor ligand links two Co²⁺ ions to form a two-dimensional (2D) plane (Fig. 1b), which are fur-

ther linked into a supramolecular 3D framework via π···π interactions involving the phenyl rings and imidazol rings of 1,4-Bib ligands with the vertical distance of 3.4796 Å (Fig. 1c), and the entire 3D topological structure can be simplified as Fig. 1d.

In structure **II**, the La(III) center is coordinated by two O atoms from two water molecules and six O atoms from five Ttac⁴⁻ ligands to form an eight-

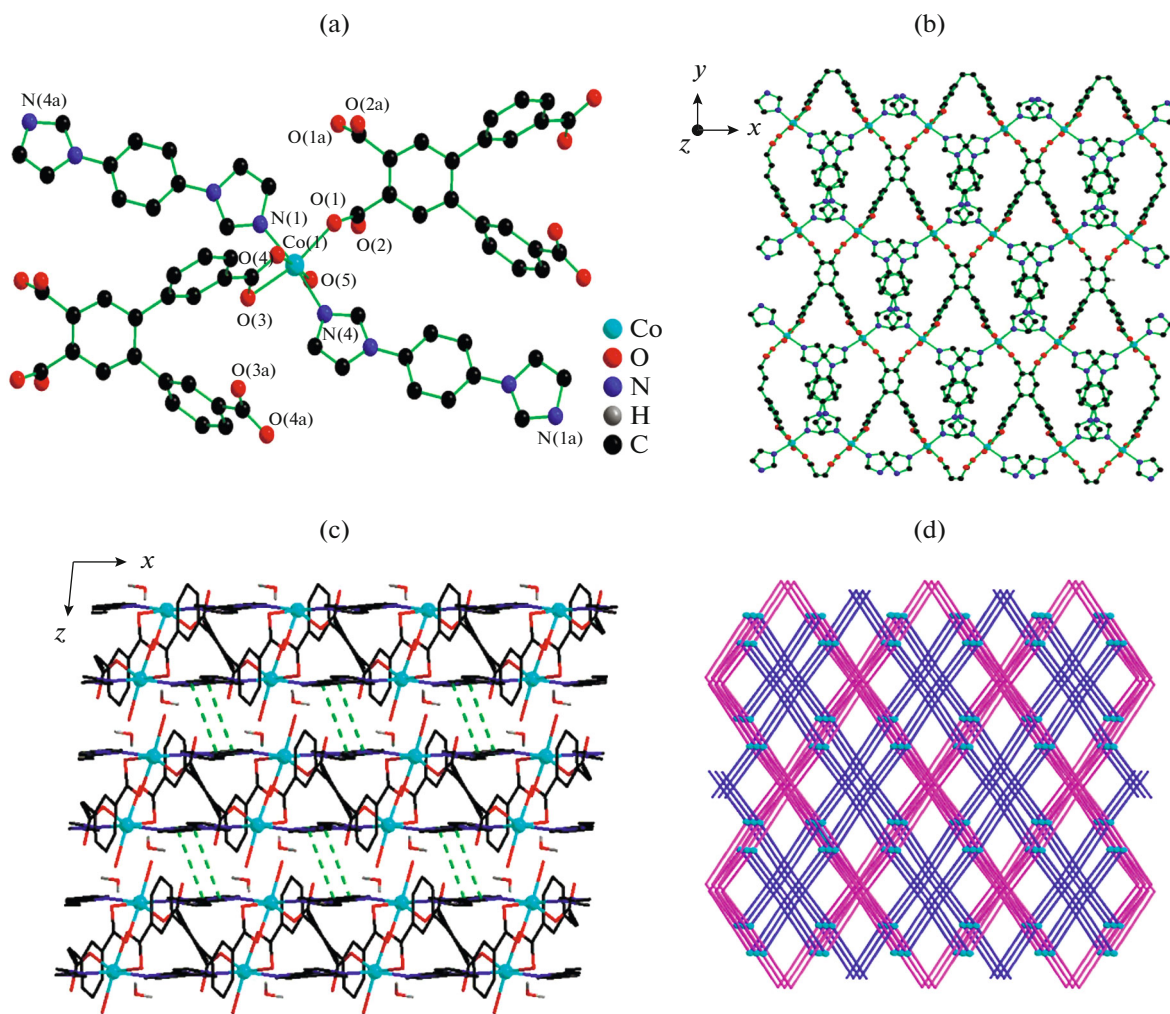


Fig. 1. The coordination environment around Co(II) in **I** (hydrogen atoms are omitted for clarity) (a); the 2D layer along z axis (b); the 3D architecture of **I** through $\pi\cdots\pi$ stacking (c); the 3D topological structure (d).

coordinated bicapped triangular prism configurations (Fig. 2a). The bond lengths of $\text{Co}-\text{O}_{\text{carboxyl}}$ are in the range 2.392–2.574 Å, the $\text{Co}-\text{O}_w$ distance is 2.542 and 2.572 Å, respectively. The angles of OLaO are within the scopes of $67.27(12)^\circ$ – $152.14(12)^\circ$ (Tables 1 and 2). In the framework, the adjacent crystallographically equivalent La^{3+} ions are bridged by two carboxyl groups in $\mu^2\text{-}\eta^1\text{:}\eta^1$ fashion to generate a 1D infinite linear chain through the linkage of two COO^- groups end to end (Fig. 2b), which are further interlinked reciprocally along y axis to give rise to a 3D framework via the covalent bonding (Fig. 2c). In addition, the lattice water molecules distributed in porous structure can form hydrogen bonds with coordinated O atoms from water and carboxyl groups Ttac^{4-} ligands (Fig. 2d), which stabilized the frameworks of **II**, and the entire 3D topological structure can be simplified as Fig. 2e.

In recent years, great efforts have been devoted to the design and construction of lanthanide MOFs (Ln-MOF) due to their excellent luminescent properties, which combine inherent porosity and guest-binding ability are rather promising for the selective recognition of ions, solvents and small molecules. The emission spectra of ligand and **II** at room temperature are showed in Fig. 3. The H_4Ttac ligand displays luminescence with an emission maximum at 432 nm upon excitation at 271 nm, which can be attributed to the intraligand electronic transition ($\pi\text{-}\pi^*$ or $n\text{-}\pi^*$); for **II** an obvious blue-shift occurs relative to free H_4Ttac ligand, there exists an intense broad emission band at 432 nm upon excitation at 268 nm. In these cases, the linker-based luminescence dominates and the blue-shifted may be ascribed to intraligand transition and charge transfer between the metal and linker [20–22].

The fluorescence life-times (τ) of the ligand and **II** are investigated in the solid state at room temperature, which obeys double-exponential decay law (Fig. 4).

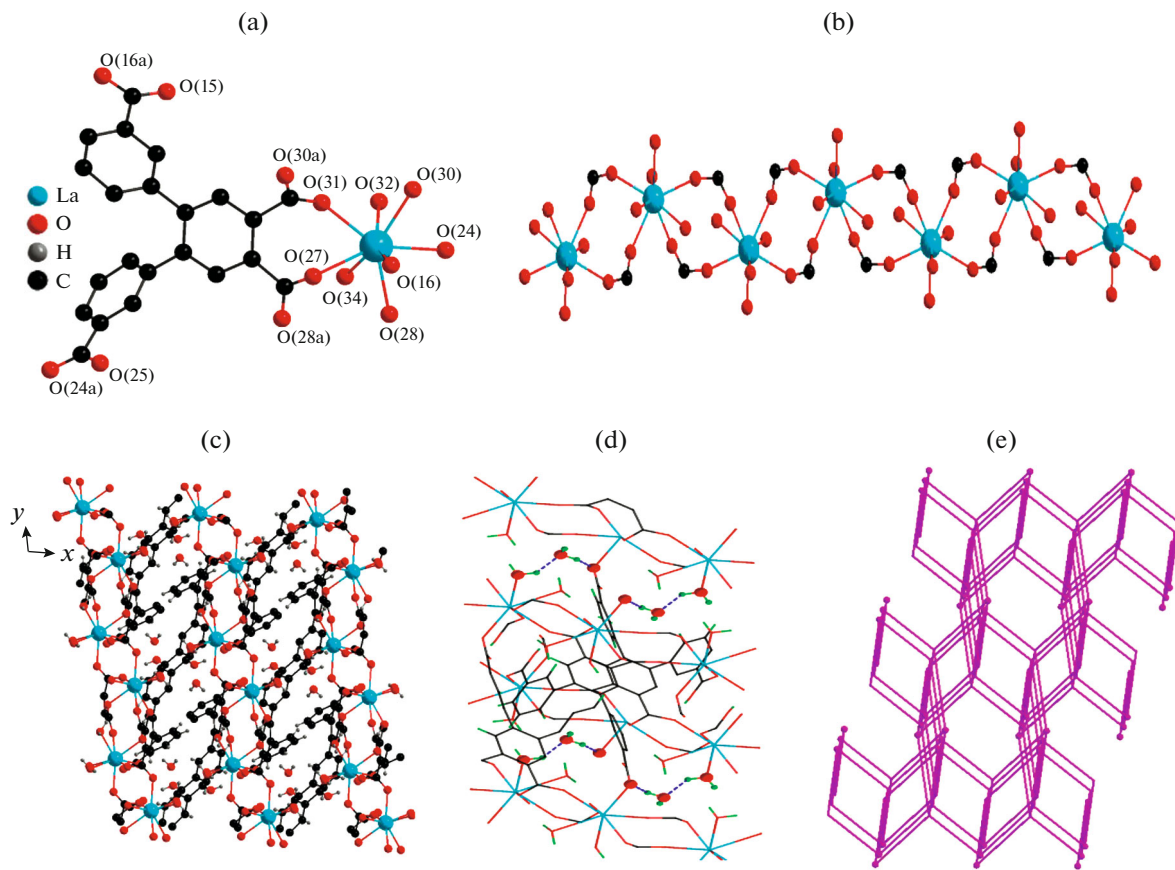


Fig. 2. The coordination environment around La(III) in **II** (hydrogen atoms are omitted for clarity) (a); the 1D wave-like chain (b); the 3D architecture of **III** along the *z* axis (c); the partial hydrogen bond (d); the 3D topological structure (e).

The fluorescence lifetime of the free organic ligand and **II** are $\tau_1 = 2.457 \mu\text{s}$ and $\tau_2 = 16.813 \mu\text{s}$ for ligand, $\tau_1 = 0.210 \mu\text{s}$ and $\tau_2 = 0.278 \mu\text{s}$ for **II**, which are much shorter than those originating from a triplet state

($>10^{-3} \text{ s}$). It is clear that the emission of light between energy states is of the same spin multiplicity. Thus, the emissions of **II** is fluorescent in nature [23, 24].

To investigate the possibilities of luminescent selective recognition of the compound towards certain metal cations, coordination polymer **II** was immersed in water solutions containing various metal cations, including Cu^{2+} ($\text{Cu}(\text{CH}_3\text{COO})_2$), Co^{2+} ($\text{Co}(\text{CH}_3\text{COO})_2$), Pb^{2+} ($\text{Pb}(\text{CH}_3\text{COO})_2$), Fe^{2+} (FeSO_4), Ni^{2+} ($\text{Ni}(\text{CH}_3\text{COO})_2$), and Mn^{2+} ($\text{Mn}(\text{CH}_3\text{COO})_2$) with the concentration of $1.0 \times 10^{-4} \text{ M}$. The luminescent emission intensities sharply decreased more than six times at the introduction of Cu^{2+} compared to that of the original coordination polymer **II**. Simultaneously, the emission intensities of coordination polymer **II** is significantly strengthen in the presence of Mn^{2+} ion for more than five times as strong as that without Mn^{2+} ion. Different from the above-mentioned, the introduction of Co^{2+} , Pb^{2+} , Fe^{2+} , and Ni^{2+} cations into the water solution of coordination polymer **II** cause only minor changes of the emission intensities (Fig. 5). As a result, coordination

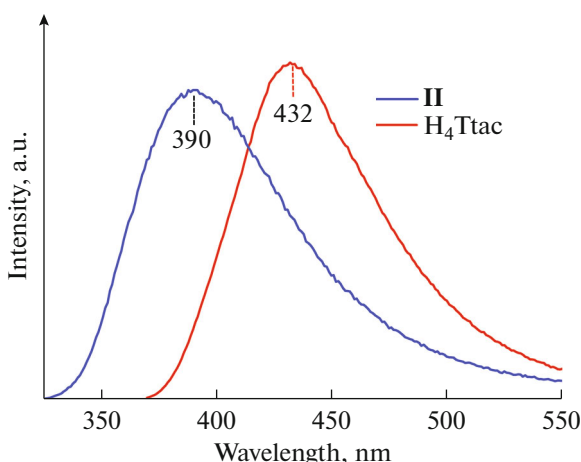


Fig. 3. The solid-state photoluminescence spectra of **II** and ligand at room temperature.

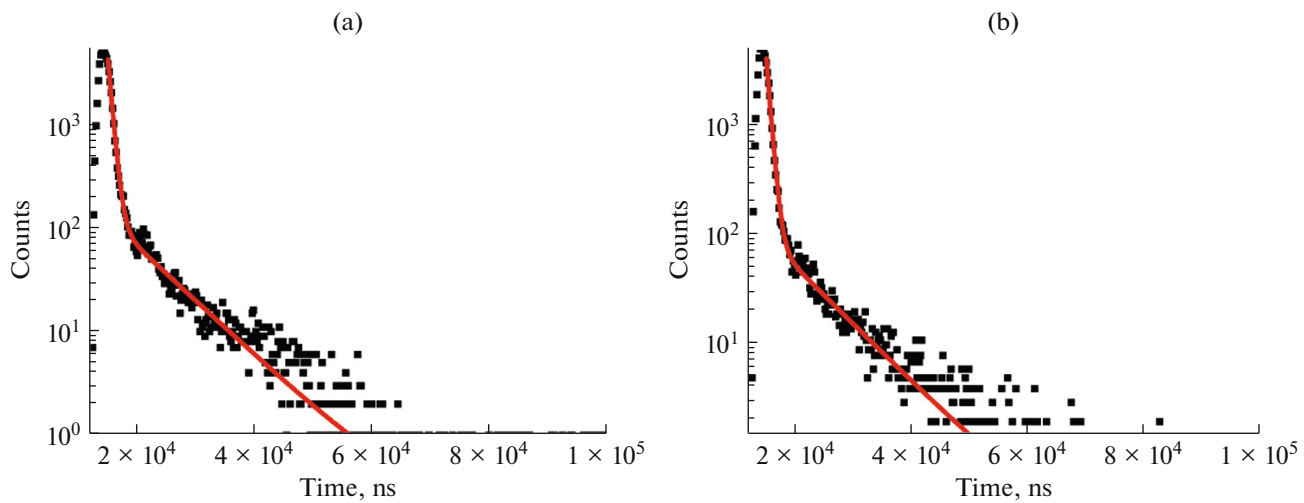


Fig. 4. The luminescence decay curve of ligand taken by monitoring the emission at 432 nm (a); the luminescence decay curve of **II** taken by monitoring the emission at 390 nm (b).

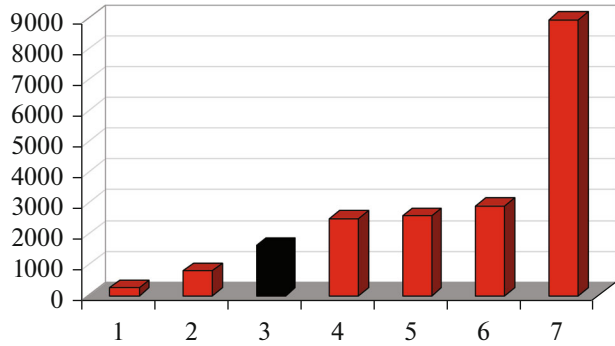


Fig. 5. The luminescent intensities of the coordination polymer **II** upon the addition of various metal cations at room temperature: Cu^{2+} (1), Co^{2+} (2), no addition (3), Pb^{2+} (4), Fe^{2+} (5), Ni^{2+} (6), Mn^{2+} (7).

polymer **II** displays good selectivity towards Cu^{2+} and Mn^{2+} ion.

ACKNOWLEDGMENTS

This work was supported by the Natural Science Foundation of Henan Province, P.R. China (nos. 162300410010 and 13A150056).

REFERENCES

1. Singh, D. and Nagaraja, C.M., *Cryst. Growth Des.*, 2015, vol. 15, no. 7, p. 3356.
2. Wang, S.L., Hu, F.L., Zhou, J.Y., et al., *Cryst. Growth Des.*, 2015, vol. 15, no. 8, p. 4087.
3. Shen, Y., Yang, X.F., Zhu, H.B., et al., *Dalton Trans.*, 2015, vol. 44, no. 33, p. 14741.
4. Kitagawa, S., *Chem. Soc. Rev.*, 2014, vol. 43, no. 16, p. 5415.
5. Gong, Y.N., Xie, Y.R., Zhong, D.C., et al., *Cryst. Growth Des.*, 2015, vol. 15, no. 7, p. 3119.
6. Liu, Y., Howarth, A.J., Hupp, J.T., et al., *Angew. Chem.*, 2015, vol. 127, no. 31, p. 9129.
7. Tobin, G., Comby, S., Zhu, N., et al., *Chem. Commun.*, 2015, vol. 51, no. 68, p. 13313.
8. Hawes, C.S., Knowles, G.P., Chaffee, A.L., et al., *Cryst. Growth Des.*, 2015, vol. 15, no. 7, p. 3417.
9. Guillerm, V., Kim, D., Eubank, J.F., et al., *Chem. Soc. Rev.*, 2014, vol. 43, no. 16, p. 6141.
10. Cui, Y., Yue, Y., Qian, G., et al., *Chem. Rev.*, 2011, vol. 112, no. 2, p. 1126.
11. Chen, D.M., Ma, X.Z., Shi, W., et al., *Cryst. Growth Des.*, 2015, vol. 15, no. 8, p. 3999.
12. Dias, S.S.P., André, V., Klak, J., et al., *Cryst. Growth Des.*, 2014, vol. 14, no. 7, p. 3398.
13. Lu, W., Wei, Z., Gu, Z.Y., et al., *Chem. Soc. Rev.*, 2014, vol. 43, no. 16, p. 5561.
14. Han, M.L., Duan, Y.P., Li, D.S., et al., *Dalton Trans.*, 2014, vol. 43, no. 46, p. 17519.
15. Tang, S.F., Pan, X.B., Lv, X.X., et al., *CrystEngComm*, 2013, vol. 15, no. 10, p. 1860.
16. Tang, R.R., Gu, G.L., and Zhao, Q., *Spectrochim. Acta, Part A*, 2008, vol. 71, no. 2, p. 371.
17. Shi, F.N., Cunha-Silva, L., Trindade, T., et al., *Cryst. Growth Des.*, 2009, vol. 9, no. 5, p. 2098.
18. Li, X.F., Han, Z.B., Cheng, X.N., et al., *Inorg. Chem. Commun.*, 2006, vol. 9, no. 11, p. 1091.
19. Aghabozorg, H., Ramezanipour, F., Kheirollahi, P.D., et al., *Z. Anorg. Allg. Chem.*, 2006, vol. 632, no. 1, p. 147.
20. Allendorf, M.D., Bauer, C.A., Bhakta, R.K., et al., *Chem. Soc. Rev.*, 2009, vol. 38, no. 5, p. 1330.
21. Zhang, C., Yan, Y., Pan, Q., et al., *Dalton Trans.*, 2015, vol. 44, no. 29, p. 13340.
22. Wang, S., Xiong, S., Wang, Z., et al., *Chem. Eur. J.*, 2011, vol. 17, no. 31, p. 8630.
23. Yang, Y., Du, P., Liu, Y.Y., et al., *Cryst. Growth Des.*, 2013, vol. 13, no. 11, p. 4781.
24. Zhang, L.P., Ma, J.F., Yang, J., et al., *Cryst. Growth Des.*, 2009, vol. 9, no. 11, p. 4660.